

# Determination of muscle architecture and fiber characteristics of the superficial and deep digital flexor muscles in the forelimbs of adult horses

Laura Zarucco, DMV, PhD; Ken T. Taylor, MS; Susan M. Stover, DVM, PhD

**Objective**—To provide a quantitative description of the architecture of superficial digital flexor (SDF) and deep digital flexor (DDF) muscles in adult horses to predict muscle-tendon behavior and estimate muscle forces.

**Sample Population**—7 forelimb specimens from 7 adult Thoroughbreds.

**Procedure**—Muscle and tendon lengths and volumes were measured from 6 fixed forelimbs. After processing, fiber bundle and sarcomere lengths were measured. Optimal fascicle lengths and muscle length-to-fascicle length, muscle length-to-free tendon length, and fascicle length-to-tendon length ratios were calculated, as were tendon and muscle physiologic cross-sectional areas (PCSAs). Pennation angles were measured in 1 embalmed specimen.

**Results**—The SDF optimal fascicle lengths were uniformly short (mean  $\pm$  SD,  $0.8 \pm 0.1$  cm), whereas DDF lengths ranged from  $0.9 \pm 0.2$  cm to  $10.8 \pm 1.6$  cm. The DDF humeral head had 3 architectural subunits, each receiving a separate median nerve branch, suggestive of neuromuscular compartmentalization. Pennation angles were small ( $10^\circ$  to  $25^\circ$ ). The PCSAs of the SDF and DDF muscle were  $234 \pm 51$  cm<sup>2</sup> and  $259 \pm 30$  cm<sup>2</sup>, with estimated forces of  $4,982 \pm 1148$  N and  $5,520 \pm 544$  N, respectively.

**Conclusions and Clinical Relevance**—The SDF muscle appears to provide strong tendinous support with little muscle fascicular shortening and fatigue-resistance properties. The DDF muscle combines passive and dynamic functions with larger tension development and higher shortening velocities during digital motion. Architectural parameters are useful for estimation of forces and have implications for analysis of muscle-tendon function, surgical procedures involving muscle-tendon lengthening, and biomechanical modeling. (*Am J Vet Res* 2004;65:819–828)

**I**n horses, the muscle-tendon complexes of the digital flexors of the forelimb are of paramount importance in

Received June 24, 2003.

Accepted October 20, 2003.

From the J. D. Wheat Veterinary Orthopedic Research Laboratory, School of Veterinary Medicine, University of California, Davis, CA 95616. Dr. Zarucco's present address is the Department of Clinical Studies, New Bolton Center, School of Veterinary Medicine, University of Pennsylvania, Kennett Square, PA 19348.

Supported by the Department of Veterinary Surgery, University of Milan, Italy, and a J. W. Fulbright grant.

Presented in part at the 30th Annual Conference of the Veterinary Orthopedic Society, Steamboat Springs, Colo, February 22–March 1, 2003.

The authors thank Dr. Cristina Sogaro, Michael Swanstrom, and Bob Parmelee for technical assistance.

Address correspondence to Dr. Zarucco.

limb function during standing and high-speed locomotion. Furthermore, efficient transfer of tension from muscular contraction to tendons via aponeurotic sheaths contributes to tendon strain and increased tendon stiffness,<sup>1</sup> with important implications for the pathogenesis of tendon diseases. Results of recent studies<sup>2,3</sup> have indicated that neither muscle nor tendon properties can be considered separately and muscle-tendon units must be regarded as an entity when trying to understand their physiologic role in locomotion events.

The architecture of a muscle is optimized for muscle function and influences both the magnitude of force that a muscle can generate and the velocity of displacement. Muscle excursion and force-generating capacity are direct functions of muscle fiber length, orientation of the muscle fiber to the axis of force generation (pennation angle,  $\alpha$ ), and physiologic cross-sectional area (PCSA). Because of these direct structure-function correlations, characterization of the muscle architecture of the superficial digital flexor (SDF) and deep digital flexor (DDF) muscles would provide insight into normal muscle-tendon functions. An understanding of the architectural specialization of these muscles may ultimately facilitate the analysis of muscle-tendon dysfunction and, hence, selection or modification of surgical procedures involving muscle-tendon lengthening (ie, accessory ligament desmotomy for treatment of flexural deformities or treatment of tendonitis), orthotics design, and forelimb biomechanical modeling.<sup>4,a,b</sup>

Muscle PCSA is indicative of the active force-generating potential of a muscle because it reflects the number of sarcomeres acting in parallel and is therefore directly related to the amount of tension that a muscle can generate. Calculation of the muscle PCSA generally incorporates muscle volume or mass divided by optimal fiber length, with or without an adjustment for the pennation angle.<sup>5-9</sup> Magnetic resonance imaging (MRI) is considered the most accurate imaging technique used presently to calculate PCSAs of human leg muscles.<sup>10,11</sup> However, MRI provides limited visualization of the length and orientation of short muscle fascicles and is of limited use in the recognition of complex muscle subdivisions<sup>12</sup> that are characteristic of the digital flexor muscles in horses.

The pennation angle is used to adjust for muscle fiber force that is not directed along the line of action of the tendon and has been determined for lower extremity muscles in humans by direct anatomic inspection of embalmed cadaveric specimens<sup>8,13,14</sup> and in vivo by means of ultrasonographic and MRI methods.<sup>10,15-17</sup>

Optimal fiber length (ie, the fiber length at which

active force is maximal) generally determines the length range and shortening velocity over which the muscle acts<sup>18</sup> and has a large effect on the sensitivity of active muscle force to tendon length changes.<sup>c</sup> There is large variation in fiber lengths in muscles of the lower extremities in humans<sup>8,13</sup> and in forelimb muscles of horses.<sup>19-24,a,d,e</sup> Muscle fiber lengths of the SDF and DDF muscles have been reported for ponies and moderate-sized and adult horses.<sup>19,20,22,23,d,e</sup> Optimal fiber lengths, pennation angles, and PCSA calculations have been reported for 9 forelimb muscles (including the SDF and DDF muscles) but only in 1 horse.<sup>a</sup> More recently, additional architectural data were obtained for the distal muscles of forelimbs in horses,<sup>20</sup> but optimal fiber lengths and detailed architectural measurements in the SDF and DDF muscles of Thoroughbreds have not been reported. The purpose of the study reported here was to provide a quantitative description of the architectural parameters of the SDF and DDF muscles in adult horses to predict muscle-tendon behavior and estimate muscle forces.

## Materials and Methods

In this study, optimal fascicle lengths (a term used instead of fiber length because small bundles of individual fibers were measured) and muscle PCSAs were determined (accounting for pennation angles), other muscle architecture ratios were calculated, and maximum force potentials were estimated for each muscle. For completeness, we also assessed the tendon parameters of both digital flexor muscles. To ascertain the influence of the architectural design of SDF and DDF muscles on their shortening velocity and tension potential, the architectural features of these muscles were examined.

**Specimen preparation**—The digital flexor muscles of the forelimbs of 1 castrated male and 6 female Thoroughbreds were used in this study; these horses were considered to have healthy SDF and DDF tendons (Table 1). Six of the 7 horses were actively in training, and all animals were euthanized for reasons unrelated to musculoskeletal disorders. Heparin sodium (200 U/kg, IV) was administered to each horse prior to euthanasia (achieved via an overdose of barbiturate administered IV); 1 forelimb was removed from each horse immediately after death (2 left and 5 right forelimbs in total) by transecting the extrinsic muscles and the humerus proximal to the origin of the extensor carpi radialis muscle. The brachial artery was cannulated above the bifurcation of the ulnar collateral artery, and the limb was secured in a custom-built frame with an adjustable loading device to reproduce the joint angles assumed during quiet postural stance (ie, 140° dorsiflexion of the elbow joint, 180° extension of the carpal joint, and 150° dorsiflexion of the metacarpophalangeal joint)<sup>25,26</sup> to derive muscle length values considered to be at functional standing length. The limb was perfused with physiologic saline (0.9% NaCl) solution via the brachial artery by use of a peristaltic pump<sup>f</sup> at a perfusion rate of 170 to 260 mL/min until complete exsanguination was achieved. Subsequently, the limb was perfused with 10% formaldehyde solution at a similar infusion rate for 40 to 60 minutes. The limb was removed from the frame, skinned, and submerged in 2% to 3% formaldehyde solution until dissected 9 to 24 months later. Because the free tendons had a tendency to partially recoil when limbs were extracted from the frame, the joint angles were remeasured in all limbs prior to dissection.

Six specimens were used for morphologic measurements of muscle and tendon length, muscle mass and vol-

ume, and fascicle and sarcomere lengths. One specimen was used to obtain fiber pennation angles.

**Morphometric measurements**—The SDF and DDF (ie, the ulnar, radial, and humeral heads and subdivisions of the humeral head) muscle-tendon units were studied in detail. Musculotendon lengths (the length of the entire muscle-tendon unit from origin to insertion) were measured in situ and after isolation from the skeleton. Muscle lengths (ie, the distance from the origin of the most proximal fibers to the insertion of the most distal fibers<sup>27</sup>) were measured along the midline on 4 surfaces (ie, cranial, medial, caudal, and lateral) of each muscle belly (ie, the SDF muscle and 3 humeral heads of the DDF muscle). Three muscle subunits (separate muscle volumes within the head) could be separated in the DDF humeral head by dissection, and individual measurements were conducted on each muscle subunit. **Free tendon lengths** ( $l^f$ ) (without intramuscular tendon) were recorded from 1 (origin tendon) or 2 (insertion tendon) surfaces (caudal or cranial and caudal, respectively) for all tendinous structures, including the **accessory ligaments of the SDF and DDF tendons** ( $AL_{SDF}$  and  $AL_{DDF}$ , respectively). They were measured from the bone origin to the proximal muscle tendon junction (origin tendon) and from the distal muscle tendon junction to either the bone insertion or the insertion on a common tendon comprised of > 1 muscle head (insertion tendon). The  $l^f$  of the DDF common tendon was measured separately.

Blotted muscle bellies and tendons were weighed, and muscle and tendon volumes were determined by water displacement to the nearest milliliter. **Cross-sectional areas** (CSAs) of common insertion tendons and accessory ligaments were calculated as the volume of the tendinous structures divided by their length.

**Muscle fiber bundle, sarcomere, and angle of pennation measurements**—The SDF and DDF muscles were prepared for fascicle determinations (length of small bundle of fibers from the tendon of origin to the tendon of insertion and sarcomere length) via a modification of described techniques.<sup>8,9,21,28</sup> The fixed muscles were placed in physiologic saline solution for 1 to 5 days to remove excess embalming chemicals. Subsequently, muscles were immersed in a 25% nitric acid solution for 2 to 4 days to soften and digest connective tissue. To slow the maceration process, the concentration of the nitric acid solution was reduced to 5% and 2.5% for an additional 1 to 2 days. When small bundles of fibers could be easily teased apart, muscles were rinsed and soaked in saline solution for 24 hours.

Ten to thirty bundles of muscle fascicles were dissected from 8 muscle regions (superficial and deep portions within proximal and distal locations) within each muscle, head, or subunit (depending on the muscle belly size) and stored in 50% glycerol. For each muscle, 240 to 280 fascicles consisting of 30 to 40 muscle fibers each were separated under a dissecting microscope and their length measured by direct macro- or microscopic observation with a resolution of 1  $\mu$ m. It was assumed that all fibers within the fascicle were of equal length, as confirmed in some samples in which individual fibers were measured. The mean **muscle fascicle length** ( $l^f$ ) for each muscle or muscle section was calculated.

Of the recorded fascicles (240 to 280), single fibers were isolated from the shortest, intermediate, and longest fascicle for each muscle and muscle head or subunit and mounted in 50% glycerol between a microscope slide and a cover glass. Fibers were viewed by use of a light microscope<sup>e</sup> and recorded with a digital video camera,<sup>h</sup> and images were stored for measurement of sarcomere length by use of a calibrated micrometer. Mean sarcomere lengths were determined by counting 10 sarcomeres from 2 to 3 regions of individual fibers for each of the 3 groups (short, intermediate,

and long fibers). **Optimal fascicle lengths** ( $l_o^M$ ) were calculated by normalizing measured mean values of  $l^F$  to a constant optimal sarcomere length ( $l^S$ ) of 2.8  $\mu\text{m}$  (the optimal sarcomere length in human leg muscle<sup>29</sup>) by use of the following equation:

$$l_o^M = l^F \times \frac{2.8}{l^S}$$

The SDF and DDF muscles from 1 forelimb (horse 7; Table 1) were fixed as described, removed from the skeleton, and frozen at  $-20^\circ\text{C}$  for 12 hours. Each muscle belly was sectioned longitudinally along the principal line of action of its tendons in 2 orthogonal planes (sagittal and dorsal). The angles formed by the orientation of intact fascicles and the line of force exerted by the origin and insertion tendons were measured with a goniometer from each muscle section on 2 planes (sagittal and dorsal) from various parts of each muscle, roughly selected proportionally to each region.<sup>14</sup> Pennation angles were measured and the mean value was calculated for each muscle, head, or subunit. The PCSA was calculated according to the following equation:

$$\text{PCSA} = (V/l^F) \times \cos \alpha$$

where  $V$  is the muscle volume based on blotted fixed muscles,  $l^F$  is the mean fascicle length for the muscle at functional standing length, and  $\alpha$  is the mean angle of pennation at that muscle length.

Table 1—Details of signalment and characteristics of 7 Thoroughbreds from which cadaveric forelimb specimens were obtained, including weight of the isolated superficial digital flexor (SDF) and deep digital flexor (DDF) muscles

Horse	Age (y)	Sex	Height at withers (cm)	Body weight (kg)	Muscle weight* (kg)		Body surface area† (m <sup>2</sup> )
					SDF	DDF	
1	10	Female	160	480	0.170	0.556	6.2
2	3	Female	NR	443	0.195	0.609	5.9
3	3	Female	168	485	0.211	0.616	6.2
4	3	Female	158	408	0.190	0.530	5.6
5	3	Female	160	512	0.250	0.731	6.5
6	3	Female	165	404	0.218	0.657	5.5
7‡	4	Gelding	165	500	NR	NR	6.4
Mean $\pm$ SD	4.1 $\pm$ 2.6		162.7 $\pm$ 3.9	461.7 $\pm$ 43.7	0.206 $\pm$ 0.030	0.617 $\pm$ 0.072	6.0 $\pm$ 0.4

\*Muscle weights are listed for formaldehyde-fixed muscles. †Body surface area is given as  $10.1 \times$  body weight (g)<sup>2/3</sup>/10,000. ‡Specimen used to measure pennation angles of the superficial and deep digital flexor (SDF and DDF, respectively) muscles. NR = Not recorded.

Table 2—Summary of muscle-tendon characteristics (mean  $\pm$  SD) for the SDF and DDF muscles obtained from 6 equine forelimbs\*

Muscle	Muscle characteristic							Free tendon length‡ (cm)	
	Muscle volume (cm <sup>3</sup> )	Muscle length (cm)	Fascicle length (cm)	Sarcomere length ( $\mu\text{m}$ )	Tendon length† (cm)	Aponeurotic tendon length (cm)	Origin	Insertion	
SDF	199.0 $\pm$ 24.0	38.8 $\pm$ 1.6	0.79 $\pm$ 0.09	2.72 $\pm$ 0.32	84.0 $\pm$ 2.6	38.1 $\pm$ 1.6	§	45.5 $\pm$ 2.0	
DDF-HH <sub>1</sub> -A	139.0 $\pm$ 18.0	28.3 $\pm$ 1.3	10.9 $\pm$ 0.8	2.85 $\pm$ 0.30	78.2 $\pm$ 3.3	17.2 $\pm$ 0.3	§	4.0 $\pm$ 1.0	
HH <sub>1</sub> -B	217.0 $\pm$ 38.0	38.8 $\pm$ 0.6	2.6 $\pm$ 0.3	2.84 $\pm$ 0.25	88.9 $\pm$ 2.2	36.9 $\pm$ 1.5	§	0.4 $\pm$ 0.6	
HH <sub>1</sub> -C	152.0 $\pm$ 12.0	33.9 $\pm$ 1.3	1.2 $\pm$ 0.1	2.44 $\pm$ 0.23	88.1 $\pm$ 1.9	32.6 $\pm$ 1.3	§	NA§	
DDF-HH (total)	508.0 $\pm$ 55.0	NA	NA	NA	NA	NA	NA	51.5 $\pm$ 1.7 (common)	
DDF-UH	80.0 $\pm$ 18.0	25.0 $\pm$ 2.7	3.9 $\pm$ 0.3	2.76 $\pm$ 0.44	92.3 $\pm$ 2.5	21.8 $\pm$ 2.7	§	19.4 $\pm$ 2.2	
DDF-RH	25.0 $\pm$ 5.0	18.1 $\pm$ 2.7	0.8 $\pm$ 0.1	2.61 $\pm$ 0.47	74.5 $\pm$ 4.0	16.6 $\pm$ 2.3	§	2.4 $\pm$ 0.5	
DDF (total)	616.0 $\pm$ 71.0	NA	NA	NA	NA	NA	NA	NA	

\*Except for DDF fascicle and sarcomere lengths which were measured in 5 forelimb specimens. †Free and aponeurotic tendon length. ‡Does not include intramuscular aponeurotic tendon length. §Absent or negligible (inconsistently measurable). ||Tendons of individual muscle heads or compartments proximal to the common insertion tendon.

SDF = Superficial digital flexor muscle. DDF = Deep digital flexor muscle. HH<sub>1</sub>-A = Humeral head compartment A (long fiber length). HH<sub>1</sub>-B = Humeral head compartment B (intermediate fiber length). HH<sub>1</sub>-C = Humeral head compartment C (short fiber length). UH = Ulnar head. RH = Radial head. NA = Not applicable.

For all muscles, heads, and subunits, the ratio of  $l^F$  to muscle length ( $l^M$ ), ratio of  $l^F$  to tendon length ( $l^T$ ), and ratio of  $l^M$  to  $l^{TF}$  (sum of all free tendon lengths) were computed. Tendon length (with intramuscular aponeurosis) was estimated by subtracting mean  $l^F$  from musculotendon length ( $l^{MT}$ ), taking the pennation angle into account<sup>30</sup> by use of the following equation:

$$l^T = l^{MT} - l^F \times \cos \alpha$$

Aponeurosis length ( $l^A$ ) was calculated as  $l^T - l^{TF}$ . Estimated maximal active isometric forces ( $F_o$ ) were calculated from the PCSA of SDF and DDF muscles by use of  $l_o^M$  values and pennation angles and assuming a maximal specific tension ( $T_s$ ) of 22.5 N/cm<sup>2</sup><sup>31</sup>:

$$F_o = \text{PCSA} \times T_s$$

All numeric data are reported as mean  $\pm$  SD. Where applicable, a 2-tailed Student  $t$  test was performed. Values of  $P < 0.05$  were considered significant.

## Results

The values reported are considered representative of trained Thoroughbreds (Table 1) with the forelimb in the standing position. The joint angles recorded prior to dissection accounted for  $138 \pm 6^\circ$ ,  $177 \pm 2^\circ$ ,

Table 3—Summary of pennation angles and calculated muscle variables in the SDF and DDF muscles obtained from 1 and 6 equine forelimbs, respectively

Muscle	Parameter					PCSA (cm <sup>2</sup> )	F <sub>0</sub> (N)*
	Pennation angle (°)	l <sub>0</sub> <sup>F</sup> (cm)	l <sup>M</sup> :l <sup>T</sup> ratio	l <sup>F</sup> :l <sup>M</sup> ratio	l <sup>F</sup> :l <sup>T</sup> ratio		
SDF	24.5 ± 3.8	0.84 ± 0.14	0.9 ± 0.1	0.02 ± 0.00	0.01 ± 0.00	234 ± 51	4,982 ± 1,148
DDF-HH <sub>1</sub> -A	10.5 ± 1.5	10.8 ± 1.6	0.5 ± 0.0	0.39 ± 0.02	0.14 ± 0.02	13 ± 2	307 ± 58
HH <sub>1</sub> -B	20.0 ± 4.0	2.6 ± 0.3	0.7 ± 0.0	0.07 ± 0.01	0.03 ± 0.00	77 ± 17	1,820 ± 404
HH <sub>1</sub> -C	22.0 ± 6.4	1.4 ± 0.2	0.6 ± 0.0	0.03 ± 0.00	0.01 ± 0.00	120 ± 15	2,313 ± 280
DDF-HH (total)	NA	NA	NA	NA	NA	197 ± 21	4,439 ± 481
DDF-UH	17.5 ± 3.5	4.0 ± 0.5	0.4 ± 0.0	0.15 ± 0.01	0.04 ± 0.00	20 ± 4	452 ± 157
DDF-RH	15.0 ± 2.1	0.9 ± 0.2	0.3 ± 0.1	0.05 ± 0.00	0.01 ± 0.00	27 ± 6	553 ± 102
DDF (total)	NA	NA	NA	NA	NA	259 ± 30	5,520 ± 544

\*Estimated maximum tetanic tension assuming a specific tension of 22.5 N/cm<sup>2</sup>.

l<sub>0</sub><sup>F</sup> = Optimal fascicle length. l<sup>M</sup>:l<sup>T</sup> ratio = Muscle length-to-free tendon length (sum of all free tendon lengths) ratio. l<sup>F</sup>:l<sup>M</sup> ratio = Fascicle length-to-muscle length ratio. l<sup>F</sup>:l<sup>T</sup> ratio = Fascicle length-to-tendon length ratio. PCSA = Muscle physiologic cross-sectional area. F<sub>0</sub> = Maximal active isometric muscle force. See Table 2 for remainder of key.

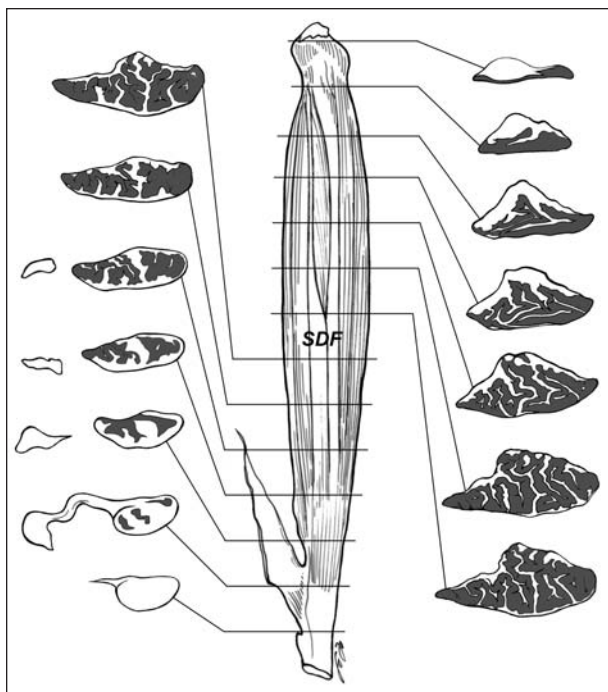


Figure 1—Illustrative drawing of the medial view of the superficial digital flexor (SDF) muscle in horses (center) with transverse sections (right and left of image) from indicated levels of transection. Internal aponeuroses (unshaded portions of sectional views) are numerous among the muscle fibers (shaded portions of sectional views).

and 160 ± 7° for the elbow, carpal, and metacarpophalangeal joints, respectively. No significant differences were observed between muscle-tendon length measurements in situ and after dissection.

#### Gross anatomic and architectural observations—

The muscle-tendon measurements and pennation angles for the SDF and DDF muscles were recorded and muscle parameters calculated (Table 2 and 3).

The SDF muscle is a single-headed, multipennate muscle of irregular triangular outline in a transverse section characterized by 8 to 12 thin connective tissue septa along the entire length of the muscle (Fig 1). The SDF muscle shares a variable number of muscle fasci-

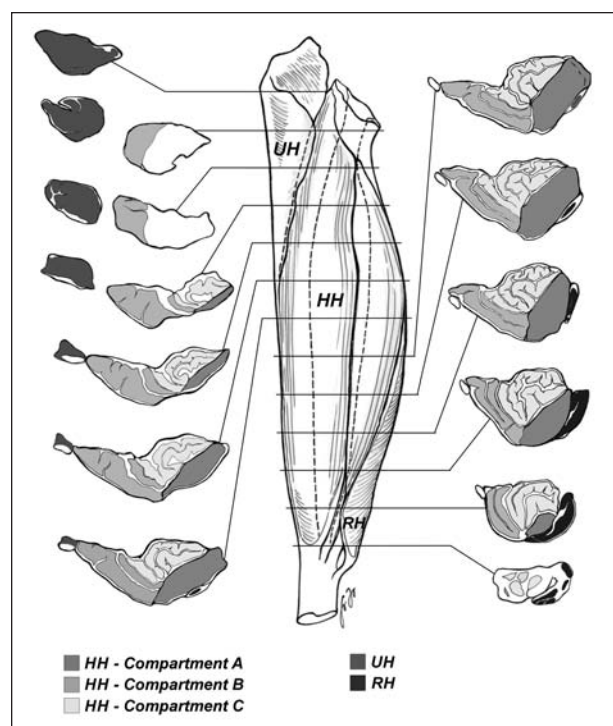


Figure 2—Illustrative drawing of the craniolateral view of the deep digital flexor (DDF) muscle in horses (center) with transverse sections (right and left of image) from indicated levels of transection. Aponeurotic tendon is indicated by unshaded areas of the sectional views. HH = Humeral head. UH = Ulnar head. RH = Radial head.

cles in the proximal third of its muscle belly with the humeral head of the DDF muscle (subunits B and C) with a common, short tendinous origin. The SDF tendon of origin is almost entirely covered by muscle fibers and continues distally in close association with the DDF muscle. Microdissection of the SDF muscle (cranial, intermediate, and caudal portions) revealed a homogeneous distribution of short fascicles (0.8 cm) with only few groups of slightly longer fibers in the proximal region.

The SDF insertion tendon constitutes approximately 54% of the total muscle-tendon length and crosses a total of 5 freely movable joints. The mean

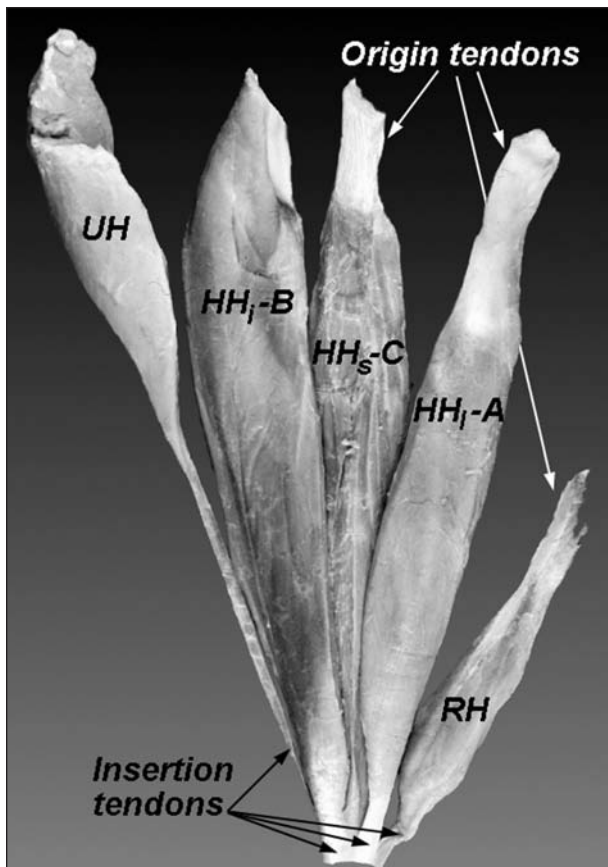


Figure 3—Photograph of the DDF muscle of a horse separated into 3 heads and 3 humeral head subunits (better defined as compartments). HH<sub>1</sub>-A = Humeral head compartment A (long fiber length). HH<sub>1</sub>-B = Humeral head compartment B (intermediate fiber length). HH<sub>1</sub>-C = Humeral head compartment C (short fiber length). The origin and insertion tendons proximal to the common distal tendon of the DDF muscle are also illustrated. See Figure 2 for remainder of key.

CSA of the SDF insertion tendon was  $1.5 \pm 0.1 \text{ cm}^2$ . The AL<sub>SDF</sub> is composed of a thicker fan-shaped fibrous band (mean length,  $7.2 \pm 1.3 \text{ cm}$ ) and a thinner sheet-like aponeurosis that blends with the periosteum of the caudal surface of the radius, medial to the radial head of the DDF muscle. The mean CSA of the AL<sub>SDF</sub> was  $1.1 \pm 0.1 \text{ cm}^2$ .

The DDF muscle is the largest muscle among the carpal and digital flexors in horses. It spans 6 movable joints and is comprised of 3 heads: the humeral, ulnar, and radial heads (Fig 2). The humeral head accounted for approximately 83% of the total DDF muscle volume, whereas ulnar and radial heads were only 13% and 4%, respectively. In the humeral head of the DDF muscle, 3 subunits (designated A, B, and C) could be distinguished (Fig 3). In all specimens examined, separate nerve branches (each originating from the proximal portion of the median nerve) entered each humeral head subunit (Fig 4), characterizing these subunits as neuromuscular compartments.<sup>32</sup> The 3 subunits (better defined as compartments) within the DDF humeral head had distinct architectural characteristics. Of the 3 compartments, the craniomedial compartment A had a unipennate architecture with the shortest muscle length (28.3 cm) and the longest mean optimal fas-

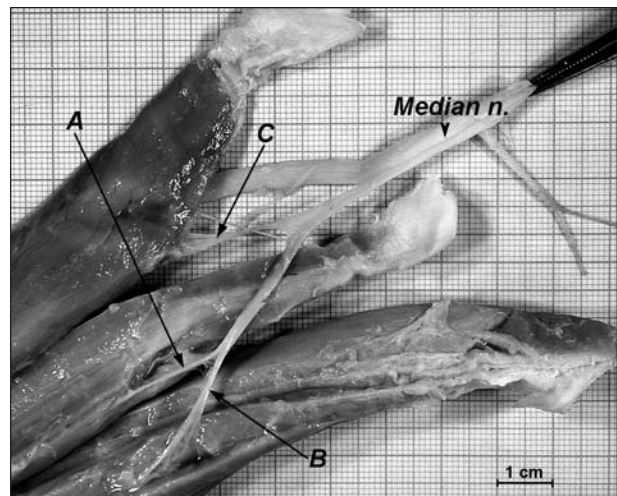


Figure 4—Photograph of the median nerve (n) branch segmentation to the 3 compartments of the DDF humeral head of a horse. A = Nerve branch to compartment A. B = Nerve branch to compartment B. C = Nerve branch to compartment C. Specimen illustrated was obtained from a young Thoroughbred that was not included in this study.

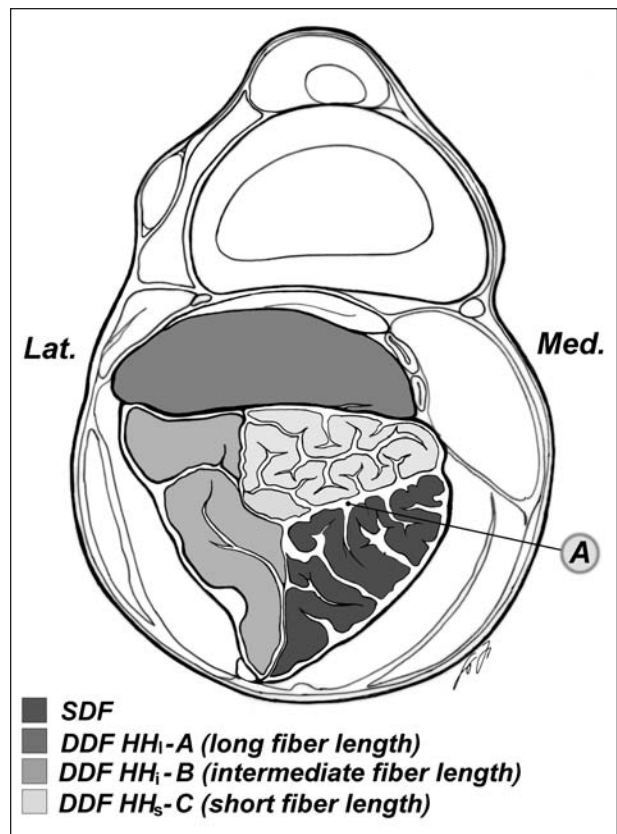


Figure 5—Illustrative drawing of a transverse section of the equine forelimb at the level of the distal third of the antebrachium. Notice the close anatomic relationship between the SDF muscle (dark-shaded) and DDF humeral head compartments C (light-shaded) and B (medium-shaded). A = Common aponeurotic tendon shared between the SDF muscle and DDF muscle compartments C and B. Lat = Lateral aspect of forelimb. Med = Medial aspect of forelimb. See Figure 3 for remainder of key.

cycle length (10.8 cm); these characteristics resulted in the highest I<sup>F</sup>:I<sup>M</sup> ratio (0.39) among the digital flexor muscle units. The lateral multipennate compartment B

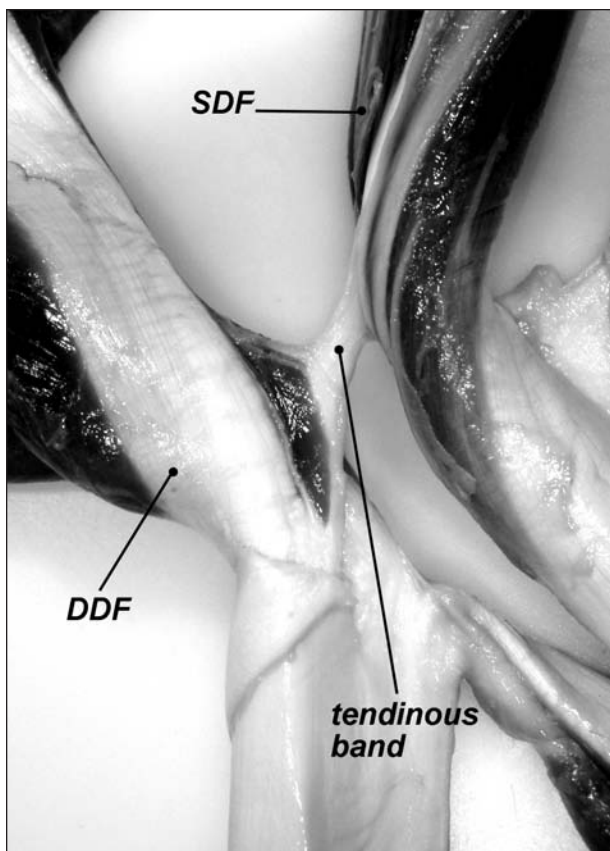


Figure 6—Photograph of the tendinous band originating from the aponeurosis of the SDF muscle (craniolateral aspect) and connected to the DDF muscle (compartments B and C) of a horse.

had the highest muscle volume (43% of the total humeral head) with the longest muscle length (38.8 cm), an intermediate mean  $l_o^M$  (2.6 cm), and the highest  $l^M:l^T$  ratio (0.7) of the 3 compartments. The middle-caudal compartment C had a multipennate architecture and very short muscle fascicles (1.4 cm) with numerous connective tissue partitions within the muscle belly, similar to the architecture of the SDF muscle with which it shares portions of a common aponeurotic septum (Fig 5). Compartments B and C are intimately associated at their origins, where muscle fibers end on common aponeuroses. Mean values of  $l^S$  were similar for compartments A and B, whereas compartment C had sarcomeres that were shorter. The DDF ulnar head had a bipennate architecture, whereas the DDF radial head had a multipennate organization with the shortest fascicles (0.9 cm) among the entire DDF muscle.

Proximal tendons of origin were measurable in the humeral compartments A and C and in the radial head. Distal tendons, proximal to the conjoined common insertion tendon, were present for humeral compartments A and B and the ulnar and radial heads. The mean CSA of the DDF common insertion tendon was  $1.89 \pm 0.1 \text{ cm}^2$ . The mean length of the  $AL_{DDFT}$  from the palmar carpal ligament to the DDF insertion tendon was  $13.7 \pm 0.4 \text{ cm}$  with a mean CSA of  $1.76 \pm 0.2 \text{ cm}^2$ .

At the flexor aspect of the proximal portion of the carpus in 3 of the 7 forelimbs, a portion of the craniolateral SDF aponeurotic tendon continued distally into a tendinous band that connected to the DDF muscle (compartments B and C; Fig 6). The tendinous band, presumably a remnant of the distal interflexorius muscle,<sup>33</sup> united the SDF and DDF muscles.

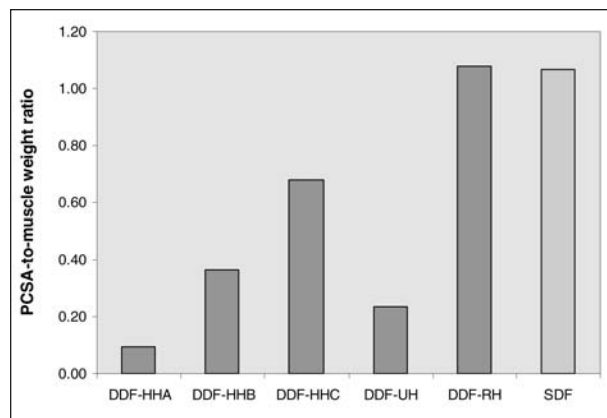


Figure 7—Histogram illustrating the ratio of physiologic cross-sectional area (PCSA) to muscle weight of individual equine muscles, heads, and compartments. A high ratio value indicates that the muscle is designed for tension production. HHA = Humeral head compartment A. HHB = Humeral head compartment B. HHC = Humeral head compartment C. See Figure 2 for remainder of key.

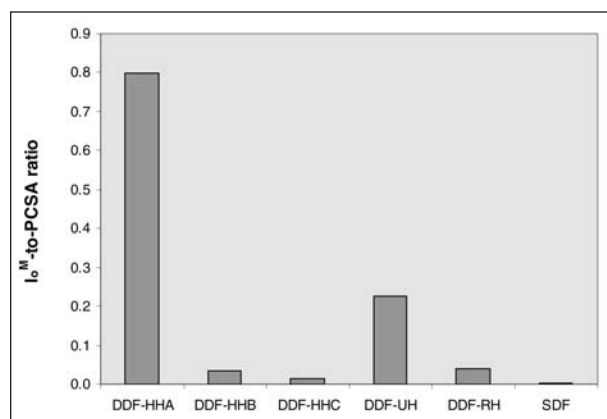


Figure 8—Histogram illustrating the ratio of mean optimal fascicle length ( $l_o^M$ ) to PCSA for individual equine muscles, heads, and compartments. A large ratio indicates that the muscle is designed for displacement or velocity of shortening. See Figures 2 and 7 for key.

lateral SDF aponeurotic tendon continued distally into a tendinous band that connected to the DDF muscle (compartments B and C; Fig 6). The tendinous band, presumably a remnant of the distal interflexorius muscle,<sup>33</sup> united the SDF and DDF muscles.

The total PCSA of the DDF muscle was  $259 \text{ cm}^2$  with the humeral head accounting for 81%. The ulnar and radial DDF heads had PCSAs of 8% and 11% of the total DDF muscle PCSA, respectively.

Pennation angles for all muscles, heads, or compartments were fairly small, with the largest angle measured in the SDF muscle ( $24.5^\circ$ ) and the lowest in compartment A of the DDF humeral head ( $10^\circ$ ).

The SDF muscle, radial head of the DDF muscle, and compartment C of the DDF humeral head had the greatest PCSA-to-muscle weight ratio (Fig 7), whereas compartment A of the DDF humeral head had the largest mean  $l_o^M$ -to-PCSA ratio (PCSA calculated with  $l_o^M$ ), with a sarcomere arrangement biased toward displacement and velocity (Fig 8).

## Discussion

The SDF and DDF muscles have a prominent biomechanical role during equine locomotion and together with their long insertion tendons and accessory ligaments constitute an important component of the passive stay-apparatus of the forelimb of horses.<sup>22</sup> In the study of this report, it was our intention to characterize and quantify the architectural properties of the SDF and DDF muscle-tendon units in an attempt to enhance our understanding of their mechanical function in equine locomotion.

The subdivision of the DDF humeral head into 3 subunits has been known for some time,<sup>33-35</sup> but the functional division of this muscle head has been previously described for only 2 main compartments (short and long).<sup>22</sup> In all forelimbs examined in the study of this report, microdissection of the 3 subunits revealed consistent differences in fascicle length among the muscle units (which is in agreement with findings of another study<sup>d</sup>) and there was distribution of a primary nerve branch to each division. The internal architecture of the DDF humeral head coupled with its compartmentalization<sup>36</sup> into 3 neuromuscular segments suggests that functional specializations could be associated with each subunit, as previously determined in other equine forelimb muscles.<sup>21,22</sup> Compartments B and C (intermediate and short fibers, respectively) of the DDF humeral head contribute substantially to total PCSA of the DDF muscle (46% and 30%, respectively) and seem to be primarily designed for tension production.<sup>13</sup> Conversely, compartment A (long fibers) undergoes considerable excursion (because the fascicle length is almost 10 times as great as that in subunits B and C) but contributed only 5% of total PCSA of the DDF muscle with a clear design for dynamic activity and higher shortening velocity. Furthermore, compartment A had the highest  $l^F:l^M$  ratio among all digital flexors, indicating a unique potential for displacement of the equine distal phalanx. Our data agreed with that of previous studies<sup>1,22</sup> regarding the role of the DDF as the primary digital flexor muscle but indicated only 1 of the DDF humeral head compartments to be the most effective flexor actuator.

In our study, the DDF muscle PCSAs were determined in young trained horses and thus avoided underestimation of muscle volume that is often associated with aging.<sup>15</sup> Computed PCSAs were larger than those previously reported<sup>20</sup> for the DDF humeral head in normal-sized horses but were similar for the entire DDF when compartmentalization was accounted for.<sup>d</sup> Additionally, values of PCSA of the humeral head compartment A in ponies<sup>23</sup> were similar to those of the Thoroughbreds examined in our study; this finding is in partial disagreement with the observation that muscle cross-sectional area scales with positive allometry in all mammalian limb muscles, except for the digital extensor muscles.<sup>37</sup> These findings emphasize that intramuscular specializations of the DDF muscle must be considered when attempting to estimate DDF forces or develop biomechanical models for the equine forelimb. Results of electromyographic and kinematic studies may help to elucidate the role of these compartments in the etiopathogenesis of flexural deformities and tendon diseases.

On the basis of fiber architecture,<sup>4,22</sup> the SDF muscle seems to be designed for tension production over a small elongation range with a total PCSA similar to that of the entire DDF muscle. In the study of this report, the mean PCSA of SDF muscles was similar to PCSA values reported for normal-sized horses<sup>20,d</sup> but greater than that reported for moderate-sized horses.<sup>23</sup> The greater compliance associated with the long, thin intramuscular aponeuroses<sup>38</sup> of the SDF muscle may partially compensate for the shortness of its muscle fibers by acting as a mechanical buffer to prevent excessive fiber lengthening and protect them from damage during eccentric contractions.<sup>39,40</sup> Similarly, the  $AL_{SDF}$  (in parallel with the SDF muscle) transfers the musculotendinous load away from the muscle belly and contributes to limiting muscle length changes.<sup>41</sup> These mechanisms appear to ensure an appropriate muscle fiber length for active tension development and potential energy absorption during high-frequency, small displacement vibration<sup>4,42</sup> following foot impact. Additionally, the SDF muscle is primarily composed of slow-twitch muscle fibers<sup>22</sup> and together with compartment C of the DDF humeral head (with which it shares a close anatomical relationship and similarity of fascicle length) could play a synergistic role<sup>28</sup> as a fatigue-resistant muscle, with high passive capacity during postural and dynamic activities. Despite the high PCSA, the architecture of the SDF muscle seems to contribute more to a somewhat passive function (ie, an active muscle with predominant tendinous function) with stretchy tendons and relatively little muscle (fascicular) shortening during locomotion.

Knowledge of SDF and DDF muscle fiber architecture is of particular importance when selecting SDF or DDF muscle-tendon lengthening surgery (eg, accessory ligament desmotomy) because such surgical procedures may negatively affect the function of those muscles<sup>43</sup> with unknown and possibly detrimental<sup>44</sup> consequences on other musculoskeletal structures.

In the study reported here, optimal fascicle lengths for the SDF and DDF muscles in forelimbs of adult horses were determined. Our morphologic data agreed well with muscle and fascicles lengths that have been determined in normal-sized horses.<sup>20</sup> Other studies assessed muscle fiber lengths in moderate-sized horses<sup>23</sup> or ponies<sup>19</sup>; those equids had body weights that were only 56% to 63% of the weight of an adult Thoroughbred and heights<sup>19</sup> that were 80% of the height of an adult Thoroughbred. Fascicle length appears to increase with horse size (ie, higher number of sarcomeres in each fiber) because fascicles in the SDF muscle and DDF humeral head compartment A from smaller horses and ponies were 38% to 75% and 46% to 57%, respectively, of the length of those fascicles in the Thoroughbreds examined in our study.<sup>19,22,23</sup> Similarly, compared with muscle and fascicle lengths in the DDF ulnar head of Thoroughbreds, the muscle and fascicle lengths in the DDF ulnar head of a pony<sup>22</sup> were only 32% and 44%, respectively. In contrast, digital flexor muscle fiber lengths of the hind limbs of mammals are reported to scale with negative allometry, particularly in muscles with very short fibers.<sup>37</sup> Discrepancies between our data and the fascicle

lengths for SDF<sup>c</sup> and DDF<sup>20</sup> muscles previously reported could be attributed to differences in the contraction state of examined muscles or the preparation techniques used (eg, fresh vs embalmed samples). The embalming method (fresh immersion fixation vs injection fixation) and the limb configuration during fixation could have also affected the measurements, particularly for the SDF muscle in which small differences in the joint angles at fixation can alter measurements of fiber length considerably.<sup>40</sup> In the study of this report, muscle specimens appeared not to shrink after excision and to be well perfused with the embalming solution without fiber fragility or breakage during measurements after maceration. Furthermore, fascicle measurements were reasonably representative of all muscle regions. In a study<sup>45</sup> of the semitendinosus muscle of horses, high variability in sarcomere lengths was detected between specimens of muscles that were in a flexed (sarcomere length, 1.67 to 1.82  $\mu\text{m}$ , fully contracted) versus an extended (sarcomere length, 2.86 to 3.11  $\mu\text{m}$ ) position (fixed by use of an in situ infiltration method); furthermore, when samples of those muscles were fixed via an immersion method, fiber contraction and kinking artifacts were observed.

Therefore, in the study of this report, measurement of sarcomere length was undertaken so that fascicle measurements were normalized or adjusted to a constant sarcomere length, which was necessary to compensate for differences in muscle length that might have occurred before or during fixation and for accurate intermuscle comparisons (because of small differences in the size of horses included in the study).<sup>46</sup> Nevertheless, even assuming a normal range of sarcomere length changes of 35%,<sup>4</sup> the differences in lengths of the DDF humeral head compartment A and ulnar head fascicles detected in our study cannot be explained without taking a geometrical scaling factor into account. Therefore, caution should be applied in the use of non-normalized fascicle length values from ponies (or small-sized horses) for musculoskeletal models or other biomechanical applications in normal-sized horses.

Comparison of the pennation angles obtained in the study of this report to those previously reported<sup>20</sup> revealed large differences. These differences were probably a consequence of the data collection method used, as suggested by the wide range of pennation angle values reported by those investigators (ie, pennation angle range in the DDF humeral head, 0° to 45°; DDF ulnar head, 5° to 35°; DDF radial head, 20° to 60°; and SDF muscle, 20° to 60°). To confirm our findings, a greater number of samples from several limbs should be examined under controlled conditions as in the present study. Although the pennation angle is an architectural parameter that is necessary for the calculation of PCSA, its influence on total muscle PCSA and maximum force output was relatively small for all muscles examined. As inferred from the equation used to calculate PCSA, the pennation angle plays a minor role in the estimate of the peak forces of SDF and DDF muscles; this is particularly obvious in the SDF muscle (largest  $\alpha$ ), which is still able to apply almost 91% of its total generated force along the direction of its insertion tendon.

The measurements of tendon lengths obtained in our study differed from values obtained in ponies<sup>19,23</sup> and ranged between 125% to 136% and 113% to 142% for SDF and DDF tendons, respectively. Tendon shrinkage as a result of fixation was previously estimated to be approximately 5%<sup>40</sup> but was not quantified in our study. All muscle units had very long tendons in both digital flexor muscles, with the lowest  $l^F:l^T$  ratios in the SDF muscle, DDF humeral head compartment C, and DDF radial head. A long tendon is functionally important with regard to the tension produced in SDF and DDF muscles; there is a different but overall high degree of tendon compliance for both muscles and a resultant storage of elastic energy within their tendons. Compared with changes in fascicle length, tendon stretching is likely to contribute more to the movement of distal joints, with higher intramuscular accommodation of changes in aponeurosis length of muscles with short fibers.<sup>47</sup>

The  $l^F:l^M$  ratio of muscles can be interpreted as a relative measure of the suitability of the muscle for excursion (high ratio) or force production (low ratio).<sup>48</sup> In the study of this report, both equine digital flexor muscles had very low  $l^F:l^M$  ratios, ranging from approximately 0.02 to 0.4 with a predominance of muscle fascicles that extended only about 4% of the total muscle length; this is much lower than that determined in digital flexor muscles in primates that require a high degree of mobility of their prehensile hands and feet.<sup>8,13,40,49</sup>

In the study of this report, computation of the estimated maximal active isometric tension in SDF and DDF muscles as a function of their PCSAs resulted in quite large values. It remains unclear why the PCSA values were so extreme. It can only be speculated that high PCSA and thus high tension development may be beneficial to increase tendon or aponeurosis stiffness (by tendon or aponeurosis lengthening) with decreased tendon compliance and more efficient storage and release of elastic strain energy. It seems feasible that the actual force-generating potential for the sarcomeres should be relatively constant even in large mammalian muscles, yet the models assumed for the transmission of sarcomere force to the tendons may be inadequate.<sup>50</sup> Thus, high force development may be differently transmitted through the muscle matrix and to aponeurotic tendons with unidentified energy uptake by the aponeurosis and less resultant force in the free tendon. Stretching of the aponeurosis could involve a further storage of elastic energy so that in the stretch-shortening cycle, more of the stored energy could be released.<sup>51</sup> The effective force generation of these muscles and the mechanism involved in the transmission of these forces to the muscle-tendon complex remain to be elucidated.

Although the potential for force generation is much greater in lengthening muscles subjected to gravitational forces<sup>52</sup> (eccentric contraction), such as the SDF and DDF muscles, PCSA alone does not strictly define a muscle's ability to generate force.<sup>50,53</sup> Other limitations related to the PCSA calculation should be taken into consideration as well. These include the number of



specimens, percentage of potential fiber shrinkage during muscle maceration,<sup>8,28</sup> unknown influence of fixation on sarcomere lengths,<sup>12</sup> assumption of homogeneity of fiber and sarcomere properties,<sup>34</sup> and possible variation in pennation angles associated with the relaxed state of cadaveric tissue or via the embalming procedure.<sup>14,15,17</sup> Additionally, when estimating muscle forces, optimization methods should be used and the muscle specific tension may not be equally assigned to all muscles. In the study of this report, the specific tension (22.5 N/cm<sup>2</sup>) that was selected was considered to be an adequate value for mixed fiber-type muscles<sup>31</sup> (such as some heads and compartments of the DDF), but it may not be entirely representative for the predominant slow, oxidative fiber composition of the SDF muscle.<sup>22</sup> If muscle stresses achieved by human flexor muscles (8 to 11 N/cm<sup>2</sup>)<sup>50</sup> and other equine muscles (8.4 ± 1 N/cm<sup>2</sup> to 12 ± 2 N/cm<sup>2</sup>)<sup>55</sup> can be < 22.5 N/cm<sup>2</sup> and not necessarily represented by a common value for all muscle units,<sup>15</sup> then the predicted muscle forces could have been largely overestimated (225% to 251%).

Our data indicated that the architectural characteristics of SDF and DDF muscles were consistent with the role of these muscles during quiet standing and high-speed locomotion. The SDF muscle design appears to contribute (with portions of DDF muscle) to a predominant tendinous support with little muscle fascicular shortening and forces developed for prolonged periods, such as those that occur during stance at rest and in locomotion. The DDF muscle fiber architecture patterns appear to be consistent with an intramuscular division of labor combining postural and dynamic functions with larger forces and higher shortening velocities during digital flexion. Our data were intended to be representative of normal-sized horses and may provide the basis for estimation of the force-generating potential of the SDF and DDF muscles with future applications for musculoskeletal limb models in Thoroughbreds.<sup>4,a,b</sup>

<sup>a</sup>Zarucco L. *Modello di simulazione computerizzata delle strutture muscoloscheletriche dell'arto anteriore equino*. PhD thesis, Clinica Chirurgica Veterinaria, Università degli Studi di Milano, Milan, Italy, 1997.

<sup>b</sup>Swanstrom MD. *Lower forelimb loading dynamics in the Thoroughbred racehorse*. PhD thesis, Graduate Group of Biomedical Engineering, College of Engineering, University of California, Davis, Calif, 2003.

<sup>c</sup>Delp SL. *Surgery simulation: a computer graphics system to analyze and design musculoskeletal reconstructions of the lower limb*. PhD thesis, Department of Mechanical Engineering, Stanford University, Palo Alto, Calif, 1990.

<sup>d</sup>Hagen R, McGuigan MP, Wilson AM. The architecture of the digital flexor muscles of the equine forelimb (abstr). *Comp Biochem Physiol B Biochem Mol Biol* 2002;132:77.

<sup>e</sup>Grandage J. Penniform muscles of the horses forelimb (abstr). *J Anat* 1981;132:318.

<sup>f</sup>MasterFlex L/S, Cole-Parmer Instrument Co, Vernon Hills, Ill.

<sup>g</sup>Olympus BH2-RFCA, Olympus America Inc, Melville, NY.

<sup>h</sup>VE 1000, DAGE-MTI of MC Inc, Michigan City, Ind.

## References

1. Ker RF, Alexander RM, Bennett MB. Why are mammalian tendons so thick? *J Zool (Lond)* 1988;216:309–324.
2. Masamitsu I, Yasuo K, Yoshiho I, et al. Nonisometric behavior of fascicles during isometric contractions of a human muscle. *J Appl Physiol* 1998;85:1230–1235.

3. Lieber RL, Brown CG, Trestik CL. Model of muscle-tendon interaction during frog semitendinosus fixed-end contractions. *J Biomech* 1992;25:421–428.
4. Wilson AM, McGuigan MP, Su A, et al. Horses damp the spring in their step. *Nature* 2001;414:895–899.
5. Brand PW, Beach RB, Thompson DE. Relative tension and potential excursion of muscles in the forearm and hand. *J Hand Surg* 1981;6:209–219.
6. Close RI. Dynamic properties of mammalian skeletal muscles. *Physiol Rev* 1972;52:129–197.
7. Crowninshield RD, Brand RA. A physiologically based criterion of muscle force prediction in locomotion. *J Biomech* 1981;14:793–801.
8. Friederich JA, Brand RA. Muscle fiber architecture in the human lower limb. *J Biomech* 1990;23:91–95.
9. Spector SA, Gardiner PF, Zernicke RF, et al. Muscle architecture and force-velocity characteristics of cat soleus and medial gastrocnemius: implications for motor control. *J Neurophysiol* 1980;44:951–960.
10. Narici MV, Landoni L, Minetti AE. Assessment of human knee extensor muscles stress from in vivo physiological cross-sectional area and strength measurements. *Eur J Appl Physiol* 1992;65:438–444.
11. Thorpe SK, Li Y, Crompton RH, et al. Stresses in human leg muscles in running and jumping determined by force plate analysis and from published magnetic resonance images. *J Exp Biol* 1998;201:63–70.
12. Delp SL, Suryanarayanan S, Murray WM, et al. Architecture of the rectus abdominis, quadratus lumborum, and erector spinae. *J Biomech* 2001;34:371–375.
13. Wickiewicz TL, Roy RR, Powell PL, et al. Muscle architecture of the human lower limb. *Clin Orthop Rel Res* 1983;179:275–283.
14. Ledoux WR, Hirsch BE, Church T, et al. Pennation angles of the intrinsic muscles of the foot. *J Biomech* 2001;34:399–403.
15. Narici MV, Binzoni T, Hiltbrand E, et al. In vivo human gastrocnemius architecture with changing joint angle at rest and during graded isometric contraction. *J Physiol* 1996;496:287–297.
16. Fukunaga T, Kawakami Y, Kuno S, et al. Muscle architecture and function in humans. *J Biomech* 1997;30:457–463.
17. Maganaris CN, Baltzopoulos V, Sargeant AJ. In vivo measurements of the triceps surae complex architecture in man: implications for muscle function. *J Physiol* 1998;512:603–614.
18. Zajac EF. Muscle and tendon: properties, models, scaling, and application to biomechanics and motor control. *CRC Crit Rev Biomech Eng* 1989;17:359–411.
19. Dimery NJ, Alexander RM, Ker RF. Elastic extension of leg tendons in the locomotion of horses (*Equus caballus*). *J Zool (Lond)* 1986;210:415–425.
20. Brown NA, Kawcak CE, McIlwraith CW, et al. Architectural properties of distal forelimb muscles in horses, *Equus caballus*. *J Morphol* 2003;258:106–114.
21. Hermanson JW, Hurley KJ. Architectural and histochemical analysis of the biceps brachii muscle of the horse. *Acta Anat* 1990;137:146–156.
22. Hermanson JW, Cobb MA. Four forearm flexor muscles of the horse, *Equus caballus*: anatomy and histochemistry. *J Morphol* 1992;212:269–280.
23. Biewener AA. Muscle-tendon stresses and elastic energy storage during locomotion in the horse. *Comp Biochem Physiol B Biochem Mol Biol* 1998;120:73–87.
24. Hermanson JW. Architecture and the division of labor in the extensor carpi radialis muscle of horses. *Acta Anat* 1997;159:127–135.
25. Holmstrom M, Magnusson LE, Philipsson J. Variation in conformation of Swedish Warmblood horses and conformational characteristics of elite sport horses. *Equine Vet J* 1990;22:186–193.
26. Stashak TS, Hill C. Conformation and movement. In: Stashak TS, ed. *Adams' lameness in horses*. Lippincott Williams & Wilkins, 2002;73–111.
27. Burkholder TJ, Fingado B, Baron S, et al. Relationship between muscle fiber types and sizes and muscle architectural properties in the mouse hindlimb. *J Morphol* 1994;221:177–190.

28. Sacks RD, Roy RR. Architecture of the hind limb muscles of cats: functional significance. *J Morphol* 1982;173:185–195.
29. Walker SM, Schrodt GR. I segment lengths and thin filament periods in skeletal muscle fibres of the Rhesus monkey and human. *Anat Rec* 1974;178:63–81.
30. Murray WM, Buchanan TS, Delp SL. The isometric functional capacity of muscles that cross the elbow. *J Biomech* 2000;33:943–952.
31. Powell PL, Roy RR, Kanin P, et al. Predictability of skeletal muscle tension from architectural determinations in guinea pig hindlimbs. *J Appl Physiol* 1984;57:1715–1721.
32. English AW, Weeks OI. Compartmentalization of single muscle units in cat lateral gastrocnemius. *Exp Brain Res* 1984;56:361–368.
33. Nickel R, Schummer A, Seiferle E, et al. Active locomotor system, muscular system, myologia In: Nickel R, Schummer A, Seiferle E, eds. *The anatomy of the domestic animals*. Berlin: Springer-Verlag Inc, 1986;214–466.
34. Bradley OC. *The topographical anatomy of the limbs of the horse*. New York: William Wood & Co, 1920;1–172.
35. Sisson S. Equine myology In: Getty R, ed. *Sisson and Grossman's: the anatomy of the domestic animals*. Philadelphia: WB Saunders Co, 1975;376–453.
36. English AW, Letbetter WD. Anatomy and innervation patterns of cat lateral gastrocnemius and plantaris muscles. *Am J Anat* 1982;164:67–77.
37. Pollock CM, Shadwick RE. Allometry of muscle, tendon, and elastic energy storage capacity in mammals. *Am J Physiol* 1994;266:R1022–R1031.
38. Lieber RL, Leonard ME, Brown CG, et al. Frog semitendinosus tendon load-strain and stress-strain properties during passive loading. *Am J Physiol* 1991;261:C86–C92.
39. Griffiths RI. Shortening of muscle fibres during stretch of the active cat medial gastrocnemius muscle: the role of tendon compliance. *J Physiol* 1991;436:219–236.
40. Alexander RM, Jayes AS, Maloiy GM, et al. Allometry of the leg muscles of mammals. *J Zool (Lond)* 1981;194:539–552.
41. Shoemaker RS, Bertone AL, Mohammad LN, et al. Desmotomy of the accessory ligament of the superficial digital flexor muscle in equine cadaver limbs. *Vet Surg* 1991;20:245–252.
42. Kingsbury HB, Qudus MA, Rooney JR, et al. A laboratory system for production of flexion rates and forces in the forelimb of the horse. *Am J Vet Res* 1978;39:365–369.
43. Savelberg HH, Buchner HH, Becker CK. Recovery of equine forelimb function after desmotomy of the accessory ligament of the deep digital flexor tendon. *Equine Vet J Suppl* 1997;23:27–29.
44. Hawkins JF, Ross MW. Transection of the accessory ligament of the superficial digital flexor tendinitis in Standardbreds: 40 cases (1988–1992). *J Am Vet Med Assoc* 1995;206:674–678.
45. Mermod L, Hoppeler H, Kayar SR, et al. Variability of fiber size, capillary density and capillary length related to horse muscle fixation procedures. *Acta Anat (Basel)* 1988;133:89–95.
46. Lieber RL. *Skeletal muscle structure and function—implications for rehabilitation and sports medicine* 1st ed. Baltimore: The Williams & Wilkins Co, 1992;1–303.
47. Huijing PA, van Lookeren Campagne AA, Koper JF. Muscle architecture and fibre characteristics of rat gastrocnemius and semimembranosus muscles during isometric contractions. *Acta Anat* 1989;135:46–52.
48. Jacobson MD, Raab R, Fazeli BM, et al. Architectural design of the human intrinsic hand muscles. *J Hand Surg* 1992;17A:804–809.
49. Lieber RL, Jacobson MD, Fazeli BM, et al. Architecture of selected muscles of the arm and forearm: anatomy and implications for tendon transfer. *J Hand Surg* 1992;17A:787–798.
50. Fukunaga T, Roy RP, Shellock FG, et al. Specific tension of human plantar flexors and dorsiflexors. *J Appl Physiol* 1996;80:158–165.
51. Ettema GJ, Huijing PA. Properties of the tendinous structures and series elastic component of EDL muscle-tendon complex of the rat. *J Biomech* 1989;22:1209–1215.
52. Gans C, Gaunt AS. Muscle architecture in relation to function. *J Biomech* 1991;24:53–65.
53. Brand RA, Pedersen DR, Friederich JA. The sensitivity of muscle force predictions to changes in physiologic cross-sectional area. *J Biomech* 1986;19:589–596.
54. Huijing PA. Muscle, the motor of movement: properties in function, experiment and modelling. *J Electromyogr Kinesiol* 1998;8:61–77.
55. Rome LC, Sosnicki AA, Goble DO. Maximum velocity of shortening of three fibre types from horse soleus muscle: implications for scaling with body size. *J Physiol* 1990;431:173–185.